INTL JOURNAL OF ELECTRONICS AND TELECOMMUNICATIONS, 2020, VOL. 66, NO. 1, PP.107-123
Manuscript received November 28, 2019; revised January, 2020. DOI: 10.24425/ijet.2020.131852

Review of Applications of the Laboratory for Electromagnetic Compatibility Infrastructure

Kamil Staniec, Zbigniew Jóskiewicz, Jarosław Janukiewicz, and Tadeusz Więckowski

***Abstract*—This article provides a thorough description of a range of non-standard application cases in which EMC laboratories can be used other than those traditionally associated with this kind of facilities. The areas covered here include investigations of: wireless and radio systems (such as IoT and broadband radio systems) also that require ultra-high operational dynamic range, emulation of interference-free and/or heavily-multipath propagation environment, shielding effectiveness of cabinets and materials (i.e. thin, light and flexible as textiles as well as heavy and thick such as building construction elements).**

***Keywords*—MIMO, IoT, GTEM cell, anechoic, semi-anechoic, reverberation, chamber, MCL, multipath, textiles, shielding effectiveness, broadband, radio**

I. Introduction to EMC Facilities

DEVELOPMENT and popularity of radio system increases a number of radio transmitters and receivers as well as occupation of another frequency bands. Together with a widespread use of many different kinds of electric and electronic devices this results in a significant increase of electromagnetic disturbance levels in our surroundings which eventually makes electromagnetic compatibility (EMC) tests impossible in that environment. Due to a high level of electromagnetic disturbances, especially those generated by radio transmitters in our environment, in some frequency ranges it is not possible to measure the electromagnetic radiation of a single device. Due to large number of radio receivers in our surroundings, that are implemented in smartphones, base stations of cellular systems, access points, tablets, laptops, TV sets as well in the newest household equipment (i.e. dishwashers and refrigerators, and many other devices), immunity tests to various electromagnetic phenomena as well as testing of new radio system are prohibited because of the possible interference of radio signal reception by these receivers or even their damage. Therefore for EMC as well as radio transmitters and receivers testing various facilities are used (i.e. chambers, cells or rooms), that provide electromagnetic separation from the outer environment and simulate inside required propagation conditions for electromagnetic fields, usually the same as in the real environment, but constrained to a limited space. It is achieved by a special design of these facilities. Shielding is provided by metal housing. Installed filters and penetration plates provide electricity, communication, remote control and fresh air, water and other media. Installed fans allow performing tests for higher field strengths. By means of the chamber shape, type, shape and arrangement of the used equipment and materials inside the chamber, radio wave propagation conditions in the chamber can be modified. Widely used in EMC tests are various kind of transmission lines (i.e. TEM cells, GTEM cells), Semi-Anechoic Chambers (SAC), Fully-Anechoic Rooms (FAR) and Reverberation Chambers (RC). Each of these EMC facilities will be presented in this paper as well as their application for alternative uses and tests.

A. The fully-anechoic room

A term "Anechoic chamber" was coined by Leo Beranek, an American acoustics expert. This term was originally used in the context of minimizing acoustics waves reflections in a room. Nowadays rooms are designed to reduce reflection for radio frequency waves too. The radio frequency anechoic room (FAR) or an anechoic chamber (FAC) is a special room designed to limit as much as possible reflection of electromagnetic waves from walls, celling, floor and other installed equipment as well as provide isolation from external electromagnetic fields. The aim of a fully anechoic chamber is to absorb energy in all directions thus simulating propagation conditions similar to those in the free space.

Reflections of radio waves are reduced by lining interior surfaces of electromagnetic screened room (Faraday's cage) with Radiation Absorbent Material (RAM). Usually RAM is a block of pyramids made of a foam or polystyrene with embedded conductive carbon black and other absorbing components. These pyramids scatter and absorb electromagnetic waves by turning its energy into a heat. The effectiveness of reducing radio waves reflection from as many incident directions as possible depends on properties and amount of the absorbing material used, its shape and size. Pyramidal RAM is most absorptive when the incident wave is at normal incidence to the internal chamber surface and the pyramid height is approximately equal to one fourth of free space wavelength. Therefore the pyramidal structures must be sized according to the wavelength. The lowest useable frequency of the FAR depends on height and type of installed pyramidal absorbers. The lower useable frequency of the FAR and better performance (higher reflection loss), the higher absorbing pyramids have to be installed. So the size and type of absorbers has to be taken into account designing the FAR to obtain required frequency range as well as size of testing volume. Increasing the height of the RAM for the same base size

This paper has been written partially as a result of realization of the following projects:
1. „ Methods and ways of protection and defence against HPM impulses" pending within strategic project: „New weaponry and defense systems of directed energy" funded by the Polish National Centre for Research and Development, the contract no. DOB-1-3/1/PS/2014.
2. The Wroclaw University of Science and Technology statutory fund no 049U/0032/19.

All Authors are with Wrocław University of Science and Technology (WUST), Poland (e-mail:{kamil.staniec}{zbigniew.joskiewicz}{jaroslaw.janukiewicz}{tadeusz.wieckowski}@pwr.edu.pl).

improves the chamber effectiveness at low frequencies but results in increased cost and a reduced unobstructed working volume available inside the chamber. High pyramids also tend to sag and tear off the walls, because the material is heavier than it looks. Especially absorbers dedicated for antenna measurement chambers (with reflection loss >35dB) have much more absorbing materials embedded than absorbers dedicated for EMC tests chambers and as a consequence are much heavier. For all these reasons FARs are designing to operate from a few hundred MHz and are usually used to perform test above 1 GHz. While the lowest frequency of the FAR depends on absorbers, the highest frequency is limited by chamber construction (shielding, filtering, ventilation), and usually is 40 GHz or more.

Special walking absorbers are used to build walkway in the FAR's floor for easy access of the staff to equipment under tested or testing apparatus. This solution allows to avoid damage or frequent disassembly of pyramidal absorbers.

To avoid the loss of absorbing materials from the foam, reduce the amount of dust and dirt in the room, and protect against fire, absorbers are painted. Different colors are used to distinguish location of doors and control panels. Yet another color is used to distinguish tips of pyramid absorbers.

When high-power tests are planned they require the use of a longer distance from transmitter to absorbers or the use of special high power air ventilated absorbers to avoid fire. Typical foam absorbers can be used for power density up to 1.5 kW/m^2. For safety reasons, inside the SAC there can be installed a gaseous fire suppression system, smoke detectors and an audio-video monitoring system.

Anechoic chambers can be any size, from a small box for the mobile phone/smartphone testing up to a hangar dedicated for trucks or aircrafts testing. There are many types of anechoic chambers that are designed for different applications. Some of the most common application are EMC tests, radiated emissions measurements (fig. 1), radiated immunity tests (also for HPEM), wireless transmitter (RF) tests, radar tests, near-field and far-field antenna as well as specific absorption rate measurements.

Installed high quality filters provide power supply for the lighting inside the FAR whereas radio signals and communication are ensured via penetration plates. For communication and remote control it is recommended to use media converters and fiber optic links. FAR has to be air-conditioned in order to keep proper environmental condition for EM absorbers.

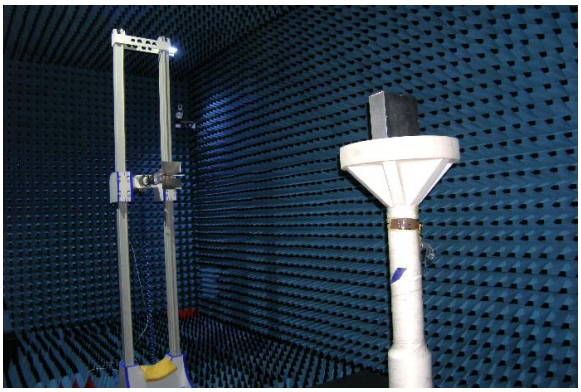

Fig. 1. Example of the test setup for radiated emissions measurement in the FAR of WUST EMC laboratory

The most important elements are positioners for mounting and manipulating the tested equipment, testing antennas or probes. Positioners provide elevation, azimuth and rotation control during the test. Because the tested equipment has to be installed in the quiet zone (without reflection), usually in the limited volume close to the center of the chamber or middle distance between two parallel walls, very important is the positioner functionality which allows easy mounting of the EUT and measuring devices (i.e. antennas, probes). Some of them can fall down but for some others the use a ladder will be necessary to install the EUT. Other auxiliary equipment depends on chamber application and implemented tested equipment.

B. The semi-anechoic chamber

The semi-anechoic chamber is a kind of the FAR with conducting floor not covered by RF absorbers to simulate the environment with propagation as over the flat and perfectly conducting earth. In this chamber radio waves reflections from the reference ground plane are required and the performance is validated by comparison to theoretical calculation. The SAC is a multifunctional test environment dedicated for commercial, military, R&D and automotive testing in frequency range from 30 MHz up to 18 GHz. Radiated emission measurements have to be performed at standardized distances of 10, 5, 3 or 1 m to receiving antenna. The maximum testing distance define chamber type. The SAC has to be much larger than FAR to allow test at specific distance and changing antenna height over the conducting floor from 1 m up to 4 m. Also the equipment tested in the SAC is usually larger and heavier than that tested in the FAR which implies that the construction of both chambers has to vary. SACs are bigger than FARs and lined with other absorber types. SACs are equipped with rotating table installed in the floor and big shielded gate to allow easy installation of a large (1.5 m × 1.5 m and more) and heavy EUT on that rotating table.

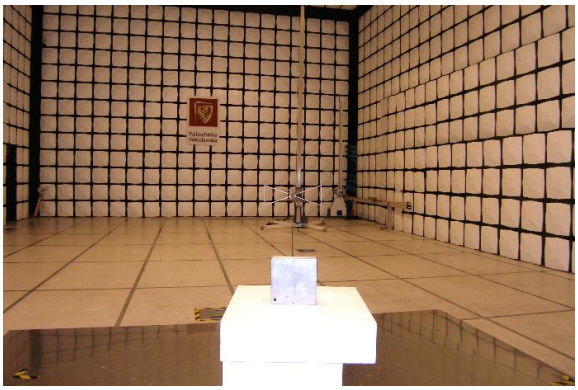

Fig. 2. Example of the test setup for radiated emissions measurement up to 1 GHz in the SAC of WUST EMC laboratory

The use of different absorbers creates a major distinction. In the SAC installed are hybrid absorbers that are combination of polystyrene or foam absorbers and ferrite plates. They operate from lower frequencies and in a wider frequency range, but are much smaller. In order to operate at 30 MHz the height of RF pyramid absorber have to be at least 2.5 m while the height hybrid absorber is less than 1 m. It allows to save some space in the SAC as well as reduce building costs. Hybrid absorbers dedicated for SAC are much cheaper and their reflection loss is lower (≥15 dB for frequencies from 30 MHz

up to 1 GHz), but sufficient to meet performance requirements defined for EMC test in SACs. It also allows to cover SAC walls only partially with absorbers or use ferrite plates only. To provide enough light in the chamber with the use of a limited number of lamps, absorbers at covered by white polystyrene caps for reflecting the light fig. 2. These caps are transparent for the electromagnetic wave measured and tested in the SAC. Tests of immunity to electromagnetic disturbances as well as radiated emission above 1 GHz have to be performed without reflection from the floor, therefore for these tests some part of floor in the SAC between antenna and the EUT has to be covered by RF absorbers: hybrid absorbers for immunity test and foam or polystyrene RF absorbers for emission tests. Also the measuring distances vary for various type of standards, so setups have to be adapted.

C. The reverberation chamber

The reverberation chamber (RC) is a spatial structure whose walls are made of metal with a very high conductivity, and the design of the entrance door, ventilation and penetrating panels ensures a very high shielding effectiveness for the electric field (fig. 3). For structural reasons, it is usually built in the form of a rectangular metal box with different dimensions of its individual sides. In this chamber, unlike with the previously presented chambers, walls are not lined with RF absorbers. High-frequency electromagnetic waves radiated inside the reverberation chamber as a result of repeated reflections from metal surfaces and relatively low energy losses, create a specific electromagnetic environment corresponding to the cavity resonator.

In order to avoid the constant and very diverse spatial distribution of the electromagnetic field inside the RC, the oscillation frequency and / or shape of the chamber and / or the location of its equipment or other elements are changed during performed tests. It is usually accomplished by using in the chamber additional movable equipment in the form of one or more rotary stirrers with installed elements for reflecting electromagnetic waves. Performed variation of the excitation frequency or chamber's configuration cause a change in the electromagnetic field distribution, ensuring statistical uniformity of the field strength in the chamber testing volume - for a full cycle of changes, e.g. frequency of the excited wave or full rotation of the stirrers.

The chamber can work in two modes of operation: tuned and stirring mode. In the tuned mode the chamber's configuration is changed in steps, i.e. stirrer is rotated in constant angle steps to the next fixed positions at which tests are performed. At least 12 steps shall be done for a full rotation. In the stirring mode the chamber's configuration is changed continuously, i.e. the stirrer is put into a continuous motion and appropriate tests have to be performed during the full rotation. Both modes are equivalent, in practice the operating mode is selected depending on the needs or it is specified in the standards [15], [22].

Other methods for changing the statistical uniformity of the EM field distribution inside the RC is by using hydraulically sliding or vibrating internal walls made of metal plates or flexible conductive materials instead of the rotating stirrer (see [25] for details). An extremely interesting solution is the use of VIRC (Vibrating Intrinsic Reverberation Chamber), made in the form of tents, whose walls vibrate as a result of moving lines attached to some corners or walls of that RC [25].

The occurrence of numerous reflections of electromagnetic waves from the walls and auxiliary equipment leads to development of a 3D standing wave inside RC which allows achieving high levels of electric field strength at relatively low excitation levels (much lower than in other chambers). Reflections allow to achieve real conditions of the electromagnetic disturbance influence on devices in the multipath propagation environment.

The chamber dimensions and volume are the key factors determining the lowest resonance frequency along with the basic mode, and as a result the chamber Lowest Useable Frequency LUF. There are various definition to determine the LUF. It can be assumed as the third multiple of the first resonance (e.g. in a cuboid chamber it can be done for frequency of $TM_{1,1,0}$ mode) or based on the minimum required number of modes.

For a cuboid reverberation chamber with dimensions L×W×H, the frequencies of individual modes are determined on the basis of the following relationship:

$$f_{l,m,n} = \sqrt{\left(\frac{l}{L}\right)^2 + \left(\frac{m}{W}\right)^2 + \left(\frac{n}{H}\right)^2}, \tag{1}$$

where: l, m, n are mode indices, and L, W, H are the chamber dimensions in [m].

It means that the larger the RC is, the lower LUF can be obtained. The stirrers efficiency and the chamber quality factor Q determine also the lowest operating frequency LUF, because adequate uniformity of the electric field strength distribution in the working volume is necessary. That requires conducting appropriate verification measurements and analysis called the chamber calibration.

The RC's upper useable frequency depends on limitations of the measuring apparatus as well as on technological limits (e.g. the RC shielding effectiveness, especially of ventilation panels, penetrating panels, door, etc.).

A remarkable advantage of the reverberation chamber is the nature of the electromagnetic environment, the largest size of the working/testing volume compared to the chamber volume and isolation of the internal electromagnetic environment from unwanted fields and signals occurring outside. Usually, the shielding effectiveness is about 100 dB, when it is made of metal elements, and about 60-80 dB for chambers made of special textile materials. Because of the lack of absorber on walls, the shielding effectiveness shall be higher than in other type of chambers. It is also important for the Q factor.

The use of rotary metal stirrers, movable or flexible walls [24], give the possibility for testing all EUT elements without changing its position or other elements of the test setup (i.e antennas, field probes). However, it is necessary to check the field statistical uniformity inside the reverberation chamber and the insertion loss between transmitting and receiving antennas when the RC is empty, each time after installing the EUT. The electromagnetic energy density at any point in the RC's test volume has a constant statistical phase, amplitude and polarization distributions for correct size, shape, arrangement, operation mode and rotation speed or number of stirrer positions. Tests are possible just after chamber calibrations. It shall be noted that measurements have to be performed in analogous conditions to those chosen during calibration. This

significantly extends the time of the measurement process. That is why the selection of the chamber calibration parameters is so important for the quality, accuracy and duration of tests. In the case of a statistical method, increasing the number of samples usually yield the more accurate results, but also significantly increase the test duration. For each laboratory, it is important to choose calibration parameters that guarantee satisfactory measurement accuracy with a minimum duration over the widest frequency range and the largest testing volume. All these features and properties of the reverberation chamber mean that it can be used not only for EMC tests.

The reverberation chamber, as any other, is an environment which can be used for testing various devices and systems. However, it is widely recognized as an alternative test setup and therefore is mainly used for testing immunity to radiated EM disturbances of military and avionics equipment [22], where high fields strength in wide frequency range are required. For the radiated emission it is necessary to convert the radiated power measured in RC to the electric field strength at specific distance for radiation in a free space or over a conducting plain. Research is currently underway and a standardization document (CISPR 16-4-5 ed. 1 Amd.2 [23]) is being developed that will allow for conversion of radiated emission limits defined for FAR and SAC to direct assessment of results obtained in the RC, which will expectedly make the use of reverberation chambers in measurements more common. A typical RC allows to conduct EMC tests in frequency range from 200 MHz (larger RCs) or 1 GHz (smaller RCs) up to 40 GHz. The use of RC for EMC tests as well as requirements and validation procedures are defined in EN 61000-4-21 standard [15].

Fig. 3. Example of the test setup with the SAC in WUST EMC laboratory

D. The GTEM cell

The GTEM cell was developed in 1984 by Asea Brown Bovery Ltd. in Switzerland [19] as a high frequency (up to several GHz) version of the TEM (Transverse Electromagnetic) cell. The GTEM cell comprises only a tapered section of the TEM cell and its enclosure has shape of a long, rectangular base pyramid therefore it is a limited length single port coaxial transmission line, stretched and terminated with a broadband RF hybrid load at one of its end. The GTEM's enclosure and inner conductor (septum) are made of conductive material, so this construction provides also electromagnetic separation from external environment and propagation of TEM mode inside as in other coaxial transmission lines. The hybrid load consists of a 50Ω distributed resistor board, that terminates the septum for lower frequencies, and pyramidal RF absorbers installed on a section of a sphere with the tips pointing towards the apex of the GTEM cell for absorbing RF energy at higher frequencies (fig. 4). This solution ensures broadband matching of this transmission line and reduces reflection from the termination. To increase working volume beneath the inner conductor, the septum is located asymmetrically within the upper third of the cell.

The GTEM is usually laid flat on the major side (bottom) and equipped with door providing access to its interior. The GTEM is a converter that allows convert RF signals at its input (apex) to TEM mode electromagnetic field (electric and magnetic field lines are orthogonal to each other and transverse to the direction of wave propagation) inside the cell and by reciprocity EM field generated inside the cell to RF signals at the input of the cell. Conversion can be done in wide frequency range (from 0Hz up to several GHz) without use of any antennas but for two components of the EM field only: radial component of electric field (field lines run from the septum to the housing) and magnetic field (lines run in circles around the septum). Conversion factor depends on the distance between septum and cell's floor, it means that depends on the EUT's location in test volume of the GTEM cell. Therefore the GTEM cell can be used for radiated immunity tests as well as radiated emission tests [20], but the EUT's location in the testing volume has to be precise defined as well as the EUT has to be rotated in other position (also orthogonal) during the test to provide coupling of all field components generated by tested device or to test immunity of all sides of the EUT to both polarization of electric or magnetic field component. All details are available in EN 61000-4-20 standard [20].

Test setup with the GTEM cell has some advantages and disadvantages [21]. It requires not too much space so can be installed in the room and is the cheapest and simplest, in comparison to other test setups. Also a few times small power is required to generate the same field strength as in the free space condition at 3 m distance (less amplification is required), and there is no need to change antennas while tests are performed in wide frequency range. Disadvantage is that the GTEM cell does not allow to test bigger devices (they have to be smaller than the wavelength and one third height between the septum and floor) and determine relative phase of the field components. Also for test, especially for emission measurement, preferred are battery operated devices, which does not change field distribution, when EUT's position is changed. Also in the GTEM cell other modes than TEM can exist, which can disturb measurement results. In this case over a limited frequency band and limited space of test volume, the field level of the longitudinal mode can be comparable or exceed the level of the intended vertical field. Test setup with the GTEM cell for immunity test to EM field is presented in fig. 4.

Fig. 4. Example of the test setup for radiated emissions measurement in the GTEM cell of WUST EMC laboratory and GTEM's interior with manipulator and installed EUT

E. Typical applications of EMC chambers

All mentioned before chambers are being mainly used for two kinds of tests performed in frequency domain: (1) measurements of radiated electromagnetic emissions of electric and electronic devices – electric or magnetic field strength at defined distance, (2) tests of immunity of electric and electronic devices to radiated electromagnetic disturbances with defined field strength values and modulation. Tests have to be performed in the frequency range of each chamber after positive validation of the test setup. Arrangement of test setup and test procedures for radiated emission of equipment use in residential, commercial and industrial environments are defined in the EN 55016-2-3 standard. Different setups are defined for measurements of E-field from 30 MHz up to 1 GHz and above 1 GHz. In both cases measurement result is maximum value of vertical and horizontal component of field strength measured for each frequency around the EUT. It means that the EUT has to be rotated in FAR (fig. 1), SAC (fig. 2) and GTEM (fig. 4). Measurement in the reverberation chamber requires rotation of the stirrer (fig. 3). Test in the SAC up to 1 GHz has to performed for various height of antenna (1m – 4m) over the floor and above 1 GHz with absorbers on the floor as in FAR (fig. 5).

Fig. 5. Example of the test setup for radiated emissions measurement above 1 GHz in the SAC of WUST EMC laboratory

Immunity tests to radiated electromagnetic disturbances are performed in the almost same test setups. In this case receiving system is being replaced by transmitting system (generator, RF amplifier and transmitting antenna). Special arrangement is required for tests in the SAC for all tested frequencies (usually above 80 MHz) – RF hybrid absorbers have to be installed between the EUT and transmitting antenna (fig. 6)

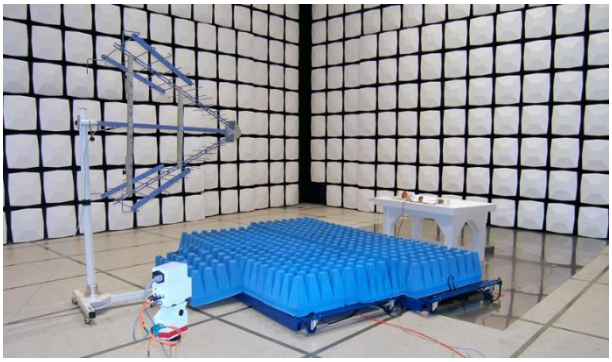

Fig. 6. Example of the test setup for immunity test to radiated EM disturbances in the SAC of WUST EMC laboratory

In SAC and RC are conducted also test which require separation from outer EM environment and additional large elements of test setup (i.e. reference ground plane). It is in case of conducted emission measurement with use of current probe according to military and avionic standards (fig. 7). Other EMC test are also performed in these chambers, usually for large and heavy equipment, when their transport to other EMC test setup is impossible or will take too much time.

In RC can be measured the shielding of device housings, cables, connectors and barrier materials, absorber properties, measuring selected antenna parameters and equivalent radiated power by radio devices. In FAR lined with high performance RF absorbers it is possible additionally to measure active and passive antenna parameters and radiation pattern in far-field as well as transmission properties of radio transmitters and receivers (using over-the-air method). With spherical scanner it is possible to measure radiation pattern of passive antenna in near-field (fig. 8).

Fig. 7. Example of the test setup for conducted emission with use of current probe according DO-160G [22] in the SAC of WUST EMC laboratory

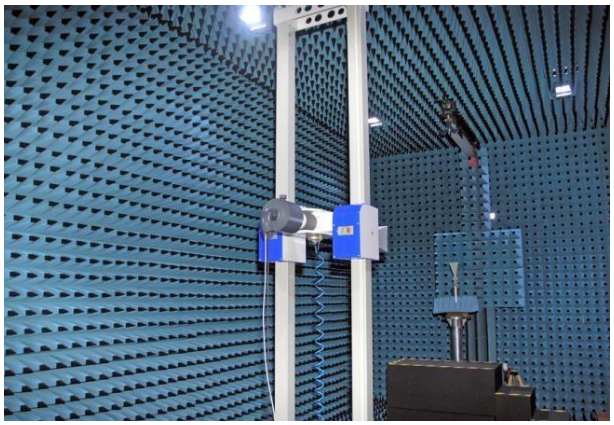

Fig. 8. Example of the test setup for antenna measurement in far-field and near-field installed in the FAR of WUST EMC laboratory

II. NARROWBAND IOT SYSTEMS INVESTIGATIONS

A. A characteristic of IoT systems

In response to the growing demand for systems surpassing sensitivity performance of traditional GPRS for handling sensor/meter traffic, a range of communication technologies have been spawned. These, termed as IoT systems, can be further subdivided into non-cellular Low-Throughput Networks (LTN) and Cellular IoT systems (see fig. 1). The former divide further into Low-Power WAN (LPWAN) [1]-[3] and Ultra-Narrowband (UNB) [4] solutions, both beyond the scope of this article. On the cellular side, three systems have been proposed

by 3GPP, of which NB-IoT is deemed to be the most optimal for mMTC (massive Machine-Type Communications) applications, especially by satisfying the following requirements set for CIoT in [5]-[6], in particular:

1. improved indoor coverage (e.g. in an apartment basement, or on indoor equipment that may be close to the ground floor etc.) extended by 20 dB compared to commercially available legacy GPRS (Non EGPRS) devices, yielding MCL of 164 dB;
2. support of massive number of low throughput devices (up to 40 per household resulting in the number of households per cell as in [6]);
3. reduced complexity and improved power efficiency allowing up to ten years battery life in UE (user equipment) with battery capacity of 5 Wh, even in locations with adverse coverage conditions, where up to 20 dB coverage extension over legacy GPRS might be needed;
4. tolerance to latency of up to several seconds.

The first requirement means that the expected sensitivities will also be low, for instance -124 dBm for NB-IoT, -136 dBm for LoRa down to -147 dBm for SigFox.

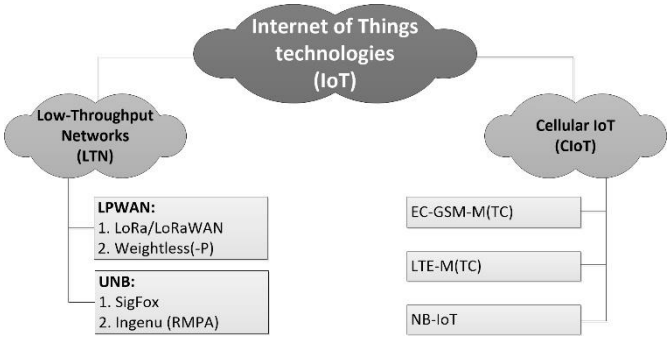

Fig. 9. The IoT ecosystem

The measurements of these systems therefore, especially near their sensitivity thresholds, pose quite a challenge and turn out to be even impossible in standard laboratories where high-class shielding effectiveness cannot be guaranteed. The reason for this impossibility is the surrounding noise and interference by far in excess of a given system target sensitivity. For this purpose one can resort to the use of shielded chambers of three types, depending on the measured phenomena, as will be extended in the following subchapters. The first type of measurements regards investigations of IoT systems' sensitivity to EM interference, which requires isolated, multipath-free conditions available in anechoic chambers (in Chapter IIB). Another sort of measurement-based investigations refers to systems that possess extremely high dynamic range of operation, i.e. 164 dB and more, appropriate conditions for which can be reproduced in a suite of connected yet mutually isolated shielded rooms (as in Chapter IIC). The last type refers to measuring an IoT system's immunity to multipath conditions, that calls for a different measurement facility, namely the reverberation chamber which reflective properties (expressed in terms of the power delay spread τ_{RMS}) can be controlled by adjusting the chamber load of absorbers, as will be demonstrated in section , as will be demonstrated in Chapter IID.

B. The use of the anechoic chamber for emulating controlled EM interference

Controlled EM interference levels can be obtained by means of placing transmit and receive antennas inside a fully anechoic chamber, with tested devices (i.e. UT – user terminal and BS – base station) located outside. The chamber itself is constructed of walls with a high shielding-effectiveness (say, 80 dB or more) for protection from outside radiation, inlaid with conical absorbers for preventing reflections. Lastly, with the interfering signal antenna put inside, the entire setup becomes suitable for measurements of highly-sensitive IoT systems, as shown schematically in fig. 10 or its physical realization in fig. 11.

In the example presented here, in order to emulate the background noise rise as a major source of wideband interference to LoRa (an exemplary IoT system), a continuous 1000-kHz wide AWGN signal was generated with the use of an arbitrary signal generator (Tektronix AWG 7000 here) with the output power P_{gen} of 7 dBm. P_{gen} was then being decreased in 3-dB steps down to -8 dBm, which allowed to observe the influence of successively increasing SNR on the resultant packet error rate which values were altering in response to changing interference power (P_{gen}) between *PER*=0% and *PER*=100%.

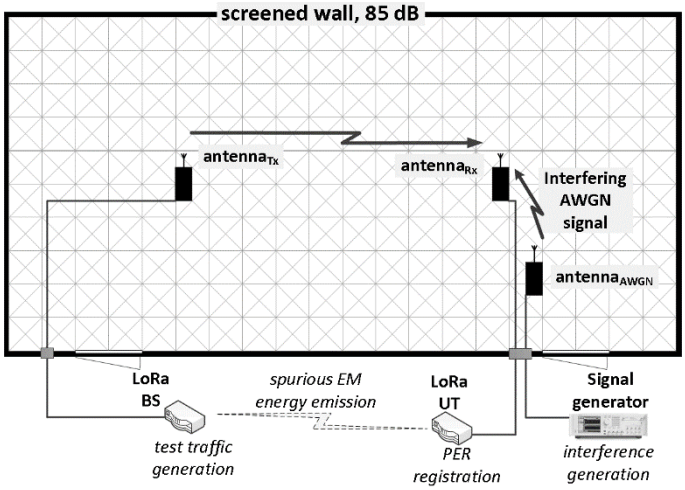

Fig. 10. The setup for sensitivity to EM interference measurements in the anechoic chamber

In the experiment the spreading factor (SF), the coding rate (*R*) and the signal bandwidth (*BW*) were also varied, that eventually led obtaining a full set of performance profiles (see fig. 12). Although LoRa is used as an example IoT system, similar profiles can be attained for any other IoT system requiring electromagnetically isolated conditions during measurements.

From the viewpoint of an IoT network planning and optimization, such profiles can turn out to be a handy tool for e.g. coverage prediction in interference-free situations as well as in situations where both the operational region and frequency bands are shared with other systems. The latter seems to be quite likely these days as most LTN IoT systems are expected to operate in the 'M' sub-band of the 868.0-868.8 MHz band [7].

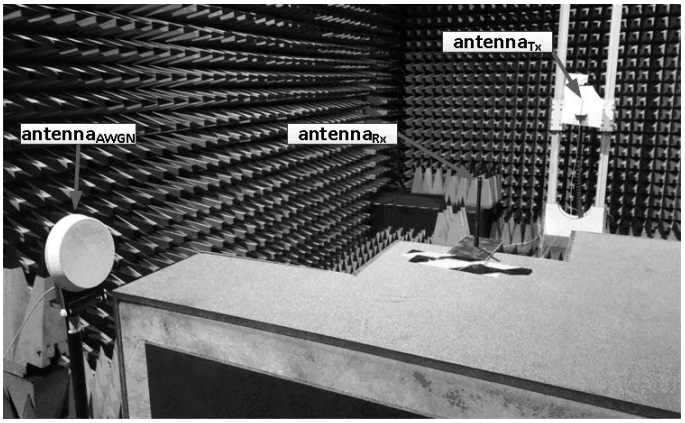

Fig. 11. The IoT ecosystem

In the case of extreme pathloss measurements, where maximum coupling losses (MCL) of 164 dB and more is required, it may be necessary to have to assemble a cable communication link that will emulate such considerable attenuation plus c.a. 10-20 dB extra space for signal detection on a spectrum analyser, which yields the total dynamic range of c.a. 185 dB. As turns out, a setup capable of achieving this figure between two ends of the signal transmission line is impossible for assembly within a single chamber by simply connecting in chain a few attenuators since parasitic radiations (coupling) from attenuators, cables and adapters connected along the line, which normally lie far below detectable power levels, will soon tend to dominate over the power levels passed through the cables causing the final signal arriving at the receiver to greatly exceed expected power levels upon reception P_{RX}.

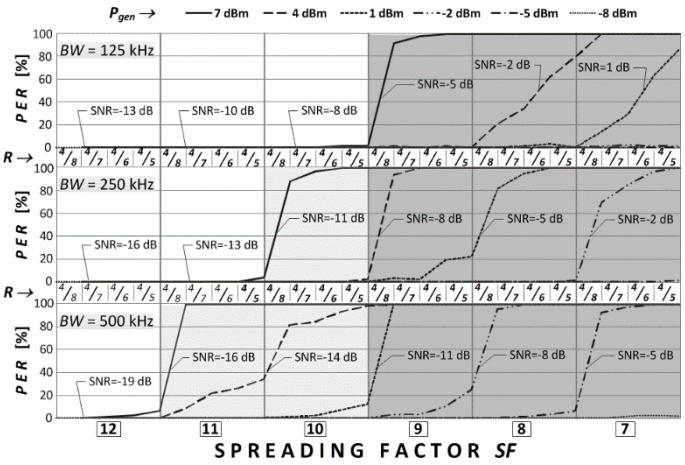

Fig. 12. Performance profiles of LoRa in response to EM interference [8]

C. The use of multiple shielded chambers for emulating extreme pathloss (MCL) conditions

A reasonable solution consists in using a signal line composed of multiple attenuation stages, each located in a separate room, electromagnetically isolated from the other rooms (or chambers).

An example setup, shown in fig. 13, assembled in WUST ECL (i.e. Wroclaw University of Science and Technology, Electromagnetic Compatibility Laboratory) included the NB-IoT base station using the transmit diversity that required the use of two separate signal lines and their final summation (combination) prior to the signal input at the receiver (i.e. the user equipment, UE).

It is noteworthy that in these situations the chambers need not be necessarily anechoic (one of them being in fact semi-anechoic) but must provide adequate isolation from one another. The presented setup therefore consists of three shielded rooms: a shielded chamber, a semi-anechoic chamber (SAC) and a shielded box wherein the UE was placed.

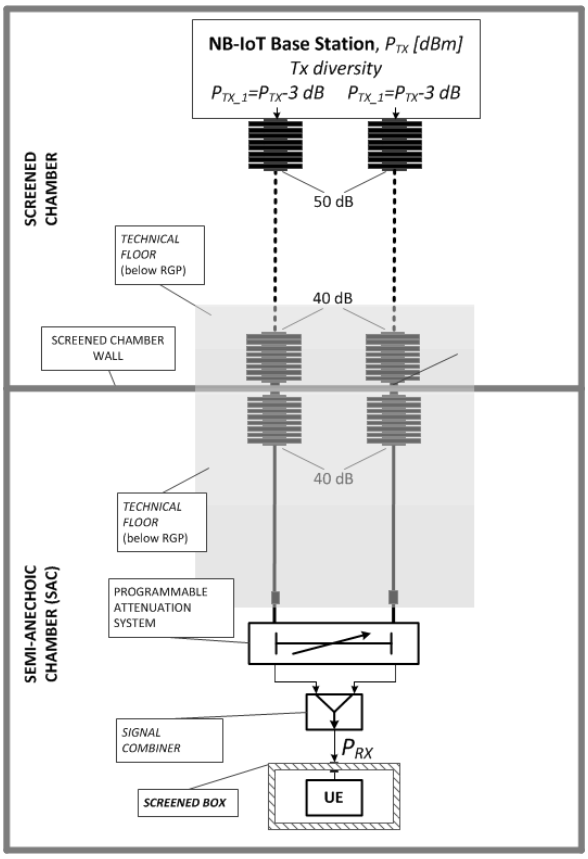

Fig. 13. Extreme pathloss measurement setup in an anechoic chamber

D. The use of a reverberation chamber for emulating controlled multipath environment

In real-world environments an emitted signal propagates via multiple interactions with its surrounding, experiencing multiple reflections from objects, transmissions through obstacles, diffractions on edges and scattering from rough surfaces or clutter. The resultant signal arrived at the receiver does not therefore appear a single instance, but as a series of echoes (i.e. copies of the original signal) with different amplitudes, phases, arrival angles and time delays. On the receiver side they are vector summed in a manner that accounts for their relative phase differences, which causes some copies to add up or cancel out, whether in-phase or counter-phase, respectively. Such behavior gives rise to, so called, small-scale fading, a typical propagation phenomenon, observed in all types of propagation environments, from indoors to open hilly terrains. The radio channel, at any point of the three-dimensional space, can be expressed as a linear, time-variant filter, or the channel impulse response $h(t,\tau)$, determined by equation (2) or, alternatively given as a Power Delay Profile (PDP) defined by formula (3). In the equation $\theta_i(t)$ and $E_i(t)$ are,

respectively, the time varying phase and the electric field amplitude of each multipath component, while τ_i is its delay. Variable channel impulse response profiles arise due to the temporal changes in the propagation surrounding, such as the motion of people, relocation of objects etc. Moreover, the radio channel is by and large also non-stationary, meaning that the *PDP* will also vary over time even when measured at precise the same location but for instance at different hours of the day.

$$h(t,\tau) = \sum_i E_i\,\delta(t-\tau_i,\tau)e^{j\theta_i(t,\tau)} \quad (2)$$

$$PDP(t,\tau) = \sum_i P_i\,\delta(t-\tau_i,\tau) \quad (3)$$

$$\tau_{RMS} = \sqrt{\frac{\sum_i(\tau_i-\tau_m)^2\cdot P(\tau_i)}{\sum_i P(\tau_i)}} \quad (4)$$

$$\tau_m = \frac{\sum_i \tau_i\cdot P(\tau_i)}{\sum_i P(\tau_i)} \quad (5)$$

A commonly accepted statistical measure of the channel time-dispersiveness is the excess time delay spread τ_{RMS} which can be interpreted as the second central moment of the *PDP*, as in formula (4), and determines the maximum symbol rate achievable by a communication system without inter-symbol interference (ISI). The most challenging propagation environments, in terms of the multipath propagation, are those with the greater values of τ_{RMS} (above 1 μs) such as hilly or mountainous areas, suburban/urban macrocells. Indoor and microcellular sites usually have τ_{RMS} on the order of dozens (indoor) or up to hundreds (in microcells) of nanoseconds.

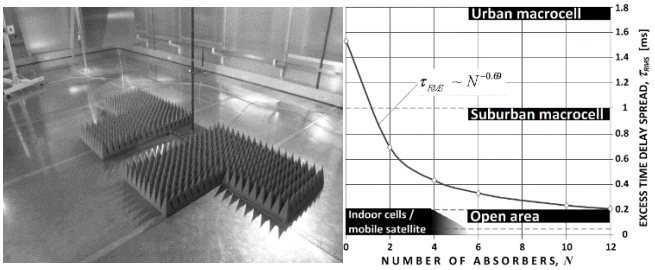

Fig. 14. left) The reverberation chamber loaded with six absorbers; right) the delay spread profile

As was demonstrated in [9], the multipath propagation can be emulated in the reverberation chamber by means of successively loading it with absorbing panels (as shown in fig. 14 left), in response to which the chamber reverberating properties will also change in the way depicted in fig. 14 (right). Thus, knowing the most probable type of environment a given system is intended to operate in, its statistical multipath properties, i.e. the time delay spread τ_{RMS}, can be reproduced (emulated) in an artificial site by loading the reverberation chamber with a number of absorbing panels that coerce its τ_{RMS} to a value corresponding to the selected propagation environment, e.g. 'Urban macrocell', 'Open area' etc., as in fig. 14 (right) where this number (N) can be obtained directly from the graphical profile. Alternatively it can be calculated from its best-fit formula relating N to τ_{RMS} obtained by means of multiple measurements performed in the reverberation chamber for various arrangements of absorbers.

It was also found in [9] that the final number of absorbers, for which the reverberation chamber was considered as overloaded, was twelve. At such a load, the delay spread obtained in the chamber would reach a stable level of ~200 ns (corresponding to indoor cells) and would remain insensitive to further increase of the load. In the unloaded case, on the contrary, i.e. with the chamber devoid of absorbers, τ_{RMS} would come up to 1.6 μs, which represents a heavily multipath environment such as urban macrocells. It should be reminded, however, that these two extremes are parameters specific to a reverberation chamber, largely dependent on its geometrical dimensions (7.76W×4.3L×3.5H meters in the case of the WUST ECL chamber).

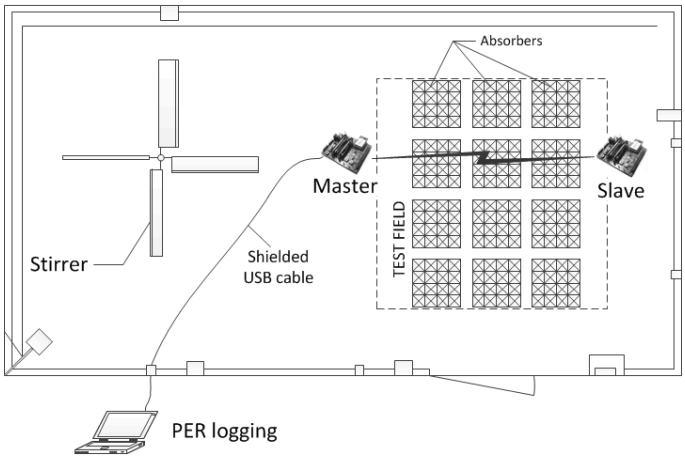

Fig. 15. A measurement setup of the reverberation chamber loaded with 12 absorbers

An exemplary application in which the reverberation chamber was used in testing performance of a communications systems in multipath conditions was ZigBee, based on the IEEE 802.15.4 specification. The investigations were performed by creating a radio link between two ZigBee devices located at the height of 54 cm above the chamber ground: one being a simple end-device (or a "slave"), the other a controller board (or a "master") possessing features allowing to perform PER tests and initiating communication sessions, as shown in fig. 15.

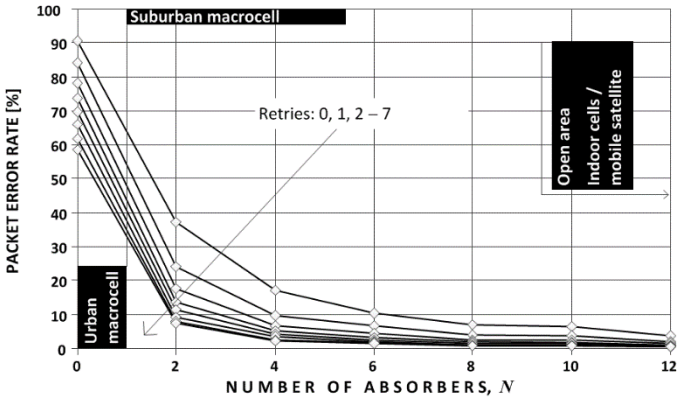

Fig. 16. ZigBee performance measurement outcomes under variable-multipath conditions of the reverberation chamber

The outcomes of measurements indicate that in the emulated environments to which ZigBee is dedicated (i.e. indoor and open spaces, both corresponding to the number of absorbers N close to overloading), the multipath propagation is rather harmless since the measured PER is below 5% in all cases (1% could be reached with a single repetition). The situation

becomes less optimistic, however, in suburban and urban macrocells in which τ_{RMS} approaches or exceeds 1 μs, respectively. In these types of environments, the use of repetitions (retries) may turn out to be necessary to keep PER low. Each of the eight curves in fig. 16 represents a single PER profile obtained for a distinct number of retries. The upmost curve represents the unacknowledged mode (i.e. without retires) whereas the bottom one represents the scenario with 7 repetitions in case of failed packet reception.

III. BROADBAND RADIO SYSTEMS INVESTIGATIONS

In response to the growing demand for fast radio data transmission new communication technologies and techniques are being developed and implemented in devices available on the market. For an end user more important is whether they are able to transfer data with declared rates in real environment and conditions. Most of devices have built in antennas therefore tests are available over-the-air only with the use of sophisticated testing devices and setups, but for new innovative devices they are not achievable. Testing the throughput in real environment usually results in a reduction of bitrate in the radio physical layer and lower transmission bitrate than the theoretical one. It could be an effect of technical and functional limitations and/or simplifications in design, but it could also be a consequence of the spectrum occupancy as well as the decrease of SNIR (Signal to Noise & Interference Ratio) due to higher interferences and/or signal attenuation (e.g. greater distance or additional attenuation brought about by objects in the radio path). Finally all these factors, supplemented by the CSMA protocol used for collision avoidance, can reduce data transmission performance of a radio system by the ARF (Automatic Rate Fallback) function, which adapts modulation and coding (MCS) schemes to the transmission quality, and. It means that performance assessment test of radio systems have to be performed in an environment with multipath propagation and fully controlled interferences and other radio transmissions.

A. *The use of a reverberation chamber for testing performance of MIMO broadband radio systems in controlled multipath environment*

As was demonstrated in the previous chapter, multipath propagation for various environments can be emulated in the reverberation chamber by means of loading the RC with some absorbing panels. The RC provides separation from other radio signals and interferences therefore was selected for investigation.

An exemplary application in which the reverberation chamber was used for testing maximum transmission rate performance of a broadband radio systems in multipath conditions, was WLAN based on the IEEE 802.11n and ac (wave 1) specifications. The investigations were performed in 2.4 GHz and 5 GHz bands by creating a radio link between two WLAN routers located in testing volume of the chamber: one being an access point, the other a client (operating in the media bridge mode) as shown in fig. 17. Separate tests were performed in the RC operating in the tuned mode for pair of ASUS RT-AC66U routers and pair of NETGEAR R6300 routers, all of them implementing MIMO 3x3 and a declared maximum transmission rates in physical layer (R_{PHY}) of 1300 Mbps. Each router was connected via a Giga-bit Ethernet interface to a laptop with running the Iperf program, exchanging datagrams using the UDP protocol.

The effect of selecting the transmission bandwidth (20MHz, 40MHz for "n" standard and additionally 80MHz for "ac" standard), UDP packet length (up to 1470 bytes), a number of absorbing panels (chamber loading and propagation environment) and stirrer position (12 with 30^0 steps) on the UDP user data rate R_{UDP} were investigated. For obvious reasons, the distance between WLAN routers did not change during the tests. Theoretical expected maximum bitrates for transmission in the 80 MHz bandwidth radio channel for IEEE 802.11ac are presented in table 1.

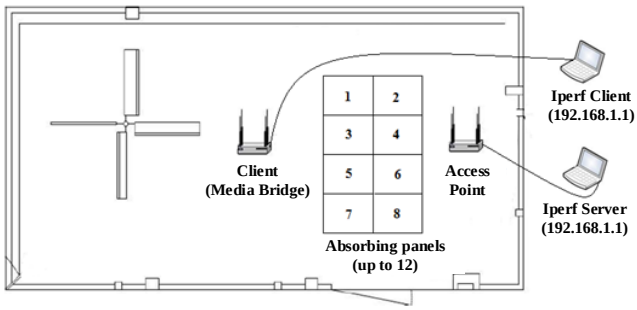

Fig. 17. A measurement setup for testing transmission performance of broadband radio systems in the reverberation chamber loaded with absorbers

The outcomes of measurements indicate that devices compatible with 802.11ac with implemented MIMO technology operate and provide data transmission in RC for all emulated environments, also in the cases corresponding to the lack and a few absorbers installed in the RC. Almost the same situation was observed for tested devices working in IEEE 802.1n standard. Only in the case of operating in 2.4 ISM band and with the lack of absorbers in the RC (without chamber loading) connection between the access point and client was not established which made the data transmission impossible. It was observed in test results of previous WLAN standards (IEEE 802.11 b, g, a) too, also when some additional absorbers were installed in the reverberation chamber.

Table 1. Examples of a theoretical expected maximum bitrates for transmission in 80 MHz radio channel acc. IEEE 802.11ac

MCS number	*MCS type*	R_{PHY} *[Mbps]*	R_{UDP} *[Mbps]*
MCS9	256QAM 5/6	1300	660
MCS8	256QAM 3/4	1170	616
MCS7	64QAM 5/6	975	507
MCS6	64QAM 3/4	877,7	456
MCS5	64QAM 2/3	780	406
MCS4	16QAM 3/4	585	304
MCS3	16QAM 1/2	390	203
MCS2	QPSK 3/4	292,5	152
MCS1	QPSK 1/2	195	101
MCS0	BPSK 1/2	97,5	50

As was depicted in fig. 18, the maximum UDP transmission data rate achieved in the RC for a full stirrer rotation depends on the transmission bandwidth, the frequency band, the number of absorbers N and their mutual arrangement. Numbers N from 1 to 12 are related to grouped absorbing panels (installed very close one to each other (fig. 19 left) and N=13 is related also to 12 absorbing panels but installed with spaces left between them (fig. 19 -right). Loading the RC with absorbers separated by spaces has a similar effect to adding an additional (i.e. 13^{th}) absorber to the grouped case of 12 panels.

The UDP data rate varies with the stirrer position (fig. 20) but in any test case the maximum data rate did not reach theoretical values.

It has to be noted that maximum UDP transmission rate can be reached by tested devices. It was confirmed by experiment performed in a real office environment.

To reach maximum transmission performance of WLAN in reverberation chamber the number of absorbing panels has to be larger than 12 (fig. 18). In this case the emulated propagation conditions in the reverberation chamber will correspond much closer to the indoor situation, based on τ_{RMS} metric (fig. 14 right), but the RC has to be overloaded. Some additional investigations have to be done to prove this thesis.

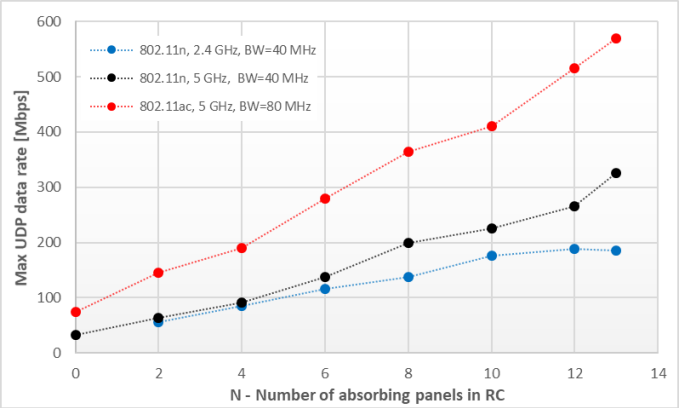

Fig. 18. UDP data transmission rate RUDP measured in the RS for ASUS RT-AC66U routers as a function of N - the number of absorbing panels

Fig. 19. Example of 12 absorbing panels installed on RC's floor: left) grouped (N=12 in fig. 18), right) separate (N=13 in fig. 18)

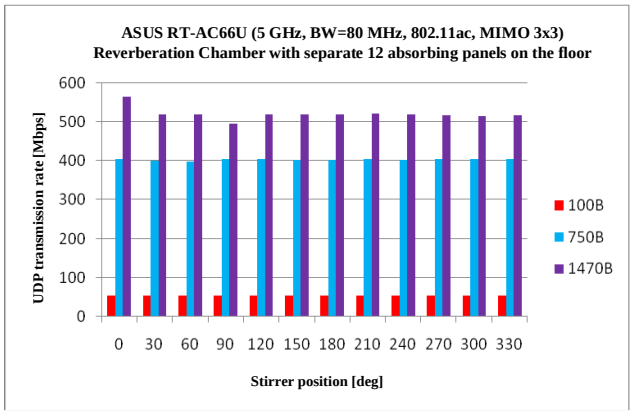

Fig. 20. UDP data transmission rate RUDP measured for ASUS RT-AC66U routers as a function of the stirrer position for separate installation of 12 absorbing panels on RC's floor

B. An artificial environment for investigating MIMO systems in semi-anechoic chamber

A full-size semi-anechoic chamber dedicated for EMC radiated emission measurement at 10 m distance from tested device as well as compact SACs, can also be used for performance testing of broadband and narrowband radio systems, especially for a direct testing of short-range systems. As was mentioned in introduction, propagation conditions in the semi-anechoic chamber are recognized as depending on direct propagation path and reflected path from the conductive floor only. Reflections from other walls are neglected because the usage of RF absorbers. This assumption is sufficient when SAC is dedicated for EMC tests only, because requirements for performance of EMC absorbers and chambers are not particularly demanding. The EMC hybrid absorbers, consisting of ferrite plates and pyramid foam or polystyrene absorbers, provide reflection loss from 15 dB to 50 dB. It means that radio waves reflected from these absorbers can be received by radio receivers, because radio systems can operate at much higher path loss attenuation. Therefore SAC guarantees controlled and reproducible environment with multi-path propagation due to reflection from the floor, but also from the walls and ceiling, which can be used for testing broadband radio systems with implemented MIMO technology. This chamber gives full separation from electromagnetic interference, and thereby elimination of the impact of other wireless devices on the measurement results. Tests can be performed for various distances between tested devices (even up to 20 m for the full-size semi-anechoic chambers), various height over the floor as well as in NLOS condition by using additional reflectors or absorbers.

Investigation have been done for a few scenarios of propagation conditions and location of WLAN routers in the SAC (fig. 21). Tests were performed using the same devices (router), their configuration and method as mentioned in the reverberation chamber study.

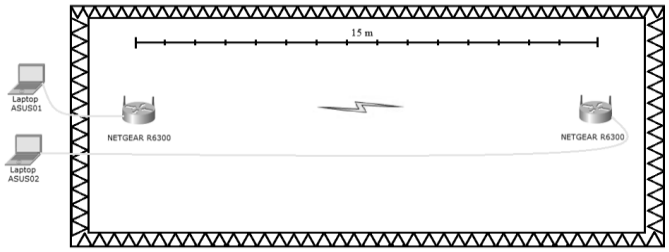

Fig. 21. A measurement setup for testing transmission performance of broadband radio systems in the semi-anechoic chamber

The effect of selecting the transmission bandwidth (20MHz, 40MHz for "n" standard and additionally 80MHz for "ac" standard), UDP packet length (up to 1470 bytes), the distance between WLAN routers (from 1 m up to 15m) and the height of both routers over the ground plane (from 0.25m up to 1 m) (fig. 22) on the UDP user data rate R_{UDP} was investigated.

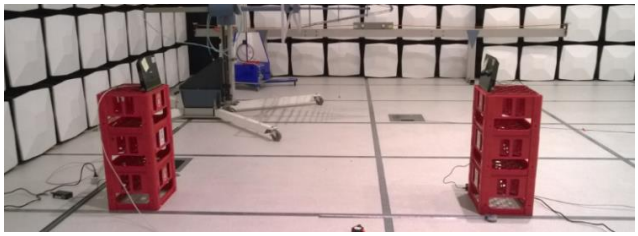

Fig. 22. An example of mutual location of tested WLAN routers (distance of 2 m and 0.75m above ground plane) during tests performed in the SAC

The measurements outcomes indicate that the data transmission performance of broadband radio systems implementing MIMO technology, especially wideband short range radio systems, can be easily tested in the semi-anechoic chamber and maximum bit rate can be measured for many scenarios. For both types of tested devices and their various configurations the maximum theoretical transmission data rates were achieved in experiments.

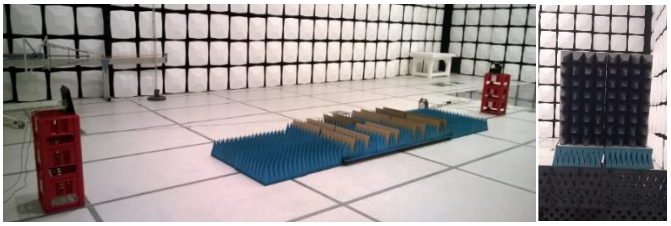

Fig. 23. Setups with used additional RF absorbers to reduce reflection from the floor and direct path propagation

In the paper presented are some measurements results for NETGEAR R6300 routers operating according to IEEE 802.11ac standard with the transmission bandwidth of 80 MHz and implemented MIMO 3x3. As was depicted in fig. 24, to determine the maximum transmission data rates for short-range broadband radio system, tested devices have to be located at the distance up to 6 m and at least 75 cm above ground plane. Much better and stable results were attained with the measuring points located in the center of the SAC rather than close to one of side longer walls (fig. 25).

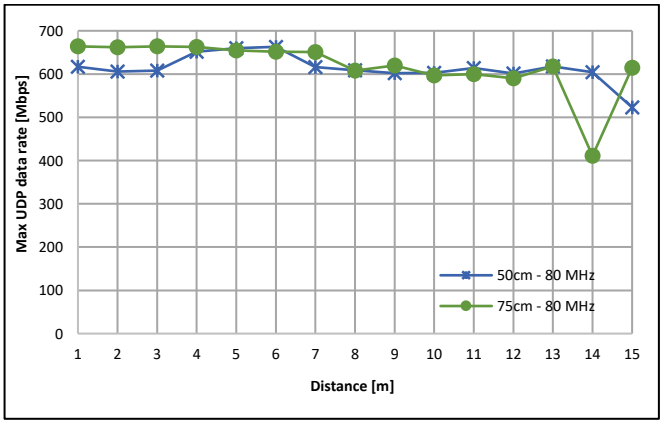

Fig. 24. UDP data transmission rate RUDP measured inside the SAC for NETGEAR R6300 routers (IEEE 802.11ac, BW=80MHz, MIMO 3x3) located 50cm and 75 cm above ground plain

Reduction of the radio wave reflection from the floor (fig. 23, left) as well as additional attenuation for direct path propagation (fig. 23, right) were emulated by installing some RF absorbers on the floor between tested devices. The outcomes of measurements (fig. 26) indicate that in both tested scenarios the emulated environments were changed leading to a decrease in UDP data rates down to about 600 Mbps, i.e. about 10% below the theoretical maximum. Still even in those cases as well as at longer distances, the transmission performance was better than in the reverberation chamber. It means that the Semi-Anechoic chamber can be considered as a testing tool for determining the transmission performance of radio systems as well as for comparing tests of various solutions and devices available on the market.

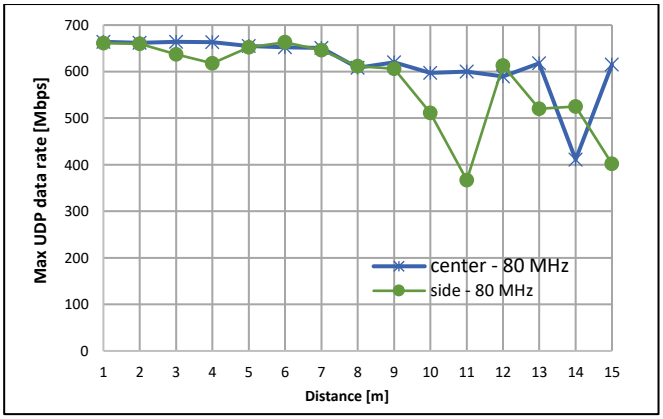

Fig. 25. UDP data transmission rate RUDP measured inside the SAC when measuring points were located in the center of the SAC and 150cm away from the side wall

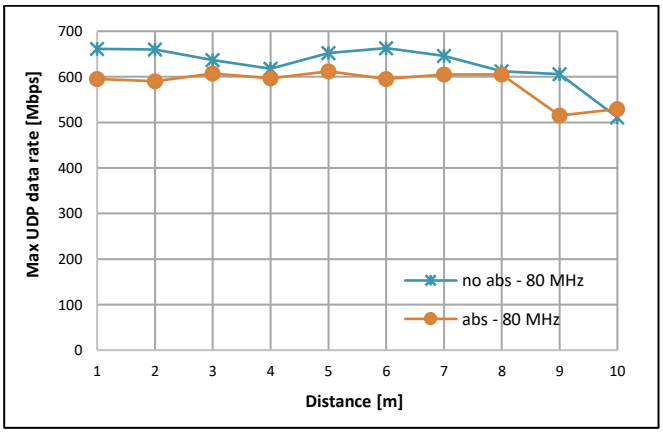

Fig. 26. UDP data transmission rate RUDP measured inside the SAC for NETGEAR R6300 routers (IEEE 802.11ac, BW=80MHz, MIMO 3x3) with use of additional RF absorbers

IV. INVESTIGATIONS OF SHIELDING PROPERTIES OF TEXTILES

A. *Shielding theory and practice*

The shielding theory is based on Maxwell's equations. The currently accepted shielding theory of an infinitely wide thin surface is based on the relations originally derived by Schelkunoff [11] in 1943. A further expansion of this theory along with many practical implementations can be found in the work of Shulz, Plantz & Brush [12]. A classical thin shields theory refers to infinitely wide monolithic fabrics of finite thickness. The fabric should be homogeneous and possess known conductivity, electric permittivity and magnetic permeability (fig. 27).

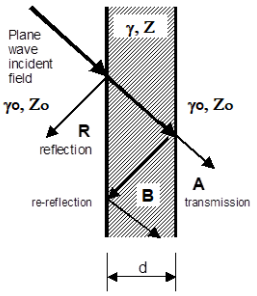

Fig. 27. Shield properties affecting shielding effectiveness

With these assumptions maintained, one can determine the shielding effectiveness of a barrier made of such a material, with the use of equations (5-10).

$$\mathrm{SE}_{dB} = 20\log_{10}\left|e^{\gamma d}\right| - 20\log_{10}|p| + 20\log\left|1 - \mathrm{q}e^{-2\gamma d}\right| \quad (6)$$

$$p = \frac{4\kappa}{(\kappa+1)^2}, q = \frac{(\kappa-1)^2}{(\kappa+1)^2}, \kappa = \frac{Z}{Z_0} \quad (7)$$

$$\gamma = \sqrt{j\omega\boldsymbol{\mu}(\boldsymbol{\sigma} + j\omega\boldsymbol{\varepsilon})} \quad (8)$$

$$Z = \sqrt{\frac{j\omega\boldsymbol{\mu}}{\sigma}} \quad (9)$$

$$\gamma_0 = j\omega\sqrt{\boldsymbol{\mu_0}\boldsymbol{\varepsilon_0}} \quad (10)$$

$$Z_0 = \sqrt{\frac{\boldsymbol{\mu_0}}{\boldsymbol{\varepsilon_0}}} \quad (11)$$

where: $\omega = 2\pi f$ – angular frequency, d – material thickness, σ – conductivity, ε, ε_0 – permittivity, μ, μ_0 – permeability, γ, γ_0 – propagation constants, Z_0 – the medium characteristic impedance.

Unfortunately, due to limited sizes of samples, the fabric inhomogeneity, difficulties with determining the electric permittivity and magnetic permeability, this theory applies directly only to the cases of solid metal shields.

Shielding defined as the ratio of the electromagnetic field intensity measured before and after installing the shielding material like fig. 28-fig. 31. It is assumed that the shield is an infinite plane and that it is placed between the source of electromagnetic radiation and the measuring device.

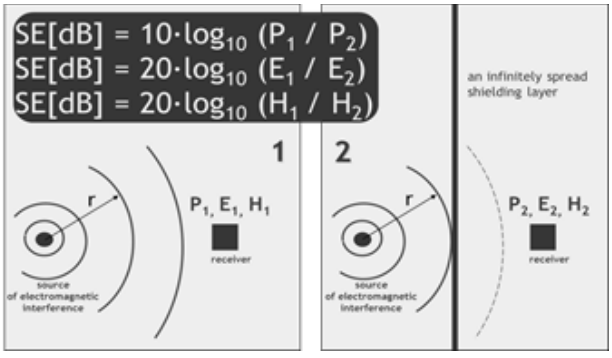

Fig. 28. Shield properties affecting shielding effectiveness

The definition of shielding effectiveness is as follows:

$$\mathrm{SE}_{dB} = 10\log_{10}\left(\frac{P_1}{P_2}\right) \quad (12)$$

$$\mathrm{SE}_{dB} = 20\log_{10}\left(\frac{E_1}{E_2}\right) \quad (13)$$

$$\mathrm{SE}_{dB} = 20\log_{10}\left(\frac{H_1}{H_2}\right) \quad (14)$$

Where the power P_1, electrical component E_1 or magnetic component H_1 are values measured without the shield, whilst the values P_2, E_2 or H_2 are measured with the shield in place. Considering the fact that in the near field wave impedance linking the electrical field strength to the magnetic field strength depends on the properties of the source of the electromagnetic field, the distance to the measurement point and the parameters of the propagation environment, shielding effectiveness in the near field will differ for the magnetic field H and the electrical field E.

There are multiple methods that allow to measure shielding effectiveness based on the above definition [16]. At present, only the ASTM D4935-10 [13] standard is dedicated to measuring the shielding effectiveness, valid over a frequency range of 30 MHz to 1.5 GHz. Moreover, methods defined in standards IEEE299 [14] and IEC 61000-4-21 [15] are sources of derivative methods for measuring shielding effectiveness. Investigations of planar materials (particularly fabrics) are carried out in WUST ECL where, due to the possessed facilities, they can be performed with the use of the most popular measurement methods, the most advanced of which is one derived from the ASTM D4935-10 standard. Research is performed in accordance with this norm as well as with modifications that allow to increase the frequency range and a better identification of material properties.

B. The ASTM D4935 method

The applied method for a plain wave allows direct measurement of the shielding effectiveness for the thin shielding material placed in the measuring adapter. The measuring adapter consists of two sections of a coaxial line terminated with a flange. The measuring instrument is a network vector analyzer enabling transmission parameters measurement.

The shielding effectiveness (*SE*) is determined as the difference between levels of attenuation measured during reference measurement (with installed reference material specimen between adapter's sections) and measurement of the sample (with installed material specimen between adapter's sections). For details see fig. 29.

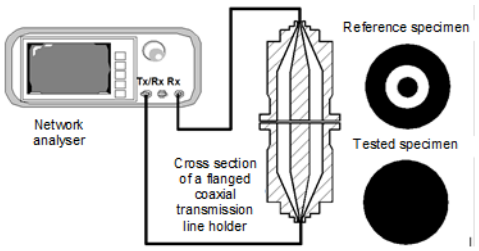

Fig. 29. Measurement test setup for a method complying with ASTM D4935.

This difference is calculated taking into account corrections determined during measurement of the reference specimen. The correction is determined because of the coupling capacity variation, which depends on the dielectric properties and the thickness of the tested material. All measurements were performed using VNA, therefore the shielding effectiveness (*SE*) was finally determined as the difference of S_{21} modules

(converted to dB), obtained from the measurement of the reference specimen (reference measurement) and from the measurement of the material sample selected for test:

$$\mathrm{SE}_{dB} = 20\log_{10}|s_{21\_ref}| - 20\log_{10}|s_{21\_se}| \qquad (15)$$

C. Modifications of the ASTM D4935-10 method

Some modifications to the ASTM D4935-10 method were adopted to provide measurements of the shielding effectiveness on larger area of tested material than the adapter surface size. Two measuring adapters were designed, called respectively F133 and F044 [17].

- F133 measuring adapter – the adapter is designed for measurements of samples with dimensions in accordance with the ASTM D4935-10 method in the frequency range from 10 MHz to 1.7 GHz. This applies to the measurement area determined by the ratio of 76 mm / 33 mm diameters of the coaxial line and flange diameter of 133 mm. The adapter construction allows to perform measurements samples with larger size as well. In the original recommendation, all adapter dimensions are indicated in inches. For the F133 adapter, all dimensions had been optimized for a metric measure system and approximately correspond to the original dimensions of the adapter presented in [13]. The adapter was designed taking into account the optimization carried out using CST simulation software to simulate full-scale electromagnetic phenomena. The Return Loss ratio is better than 22 dB over the entire measurement range.
- F044 measuring adapter - the adapter allows to extend the measuring range of the ASTM D4935-10 method to 9 GHz. The measuring area is determined by the ratio of the diameters of the external and internal wires (14 mm / 6 mm) and the collar with a diameter of 44 mm. Adapter's construction allows to perform measurements samples with larger size as well. The measurement methodology is similar to that recommended by ASTM D4935-10 with a smaller sample area. The frequency range extends from 10 MHz to 9 GHz. The adapter is designed taking into account the optimization carried out using CST simulation software. The Return Loss factor is at least 23 dB in the entire measurement range.

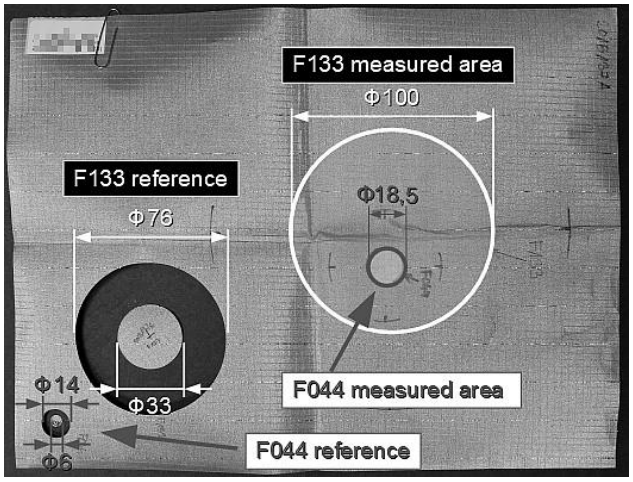

Fig. 30. Material sample prepared for shielding effectiveness measurement with marked positions of the F044 and F133 adapters.

In the applied method, measurements are performed 5 times on different areas of the sample's surface. Measuring area is limited by a circle with a diameter about 100 mm when the adapter F133 is used, and with a diameter about 18.5 mm for F044 adapter use case. If the sample size is smaller mentioned circles and larger than adapter's surface size, single measurement is performed only. Example of prepared sample see fig. 29.

Measurements were conducted according following test plan:

1. Preparation of a reference specimen as well as sample for measurement;
2. Full photographic documentation of the tested samples;
3. Determining of the measurement frequency range in the vector network analyzer;
4. Selection measured parameters of the VNA: frequency range, power of transmitted signal, RBW, registered parameters and the method of displaying measurement results;
5. Calibration at the ends of coaxial cables, which will be used to connect the measuring adapter to VNA;
6. Connection of the adapter to the network analyzer using calibrated coaxial cables;
7. Measurement of *S* parameters matrix (S_{11}, S_{21}, S_{12}, S_{22}) for an empty adapter (without any sample);
8. Measurement of *S* parameters matrix for a sample with very high shielding effectiveness (determination of the dynamics of the measuring system);
9. Measurement of *S* parameters matrix for a reference specimen;
10. Measurement of S parameters matrix for the sample of tested material;
11. Repeating point 10 for all planned positions of the measurement adapter on surface of material sample selected for tests;
12. Processing of registered results into a common format;
13. Preparation of measurement results and preparation of the test report.

For steps from 5 to 11 indicated in algorithm presented above, the obtained measurement results are recorded as files in *.s2p format. These files containing the coefficients of the S scattering matrix as a function of the frequency. Additionally screenshots of VNA as the *.png format files are recorded.

Steps from 3 to 12 are controlled by scripts launched in the Scilab [18] environment.

Fig. 31. Test setup used for reference measurement with use of F133 adapter

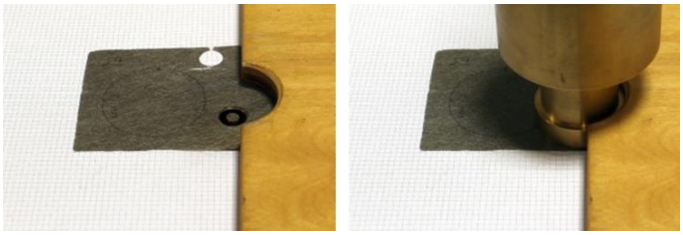

Fig. 32. Test setup used for reference measurement with use of F044 adapter

During the reference measurement, the adapter was positioned centrally in the location of the cut-out hole, as shown in fig. 30. Between inner electrodes of both adapter's sections was located cut disc of 33 mm diameter for the F133 (fig. 31) adapter or 6 mm diameter for the F044 adapter (fig. 32).

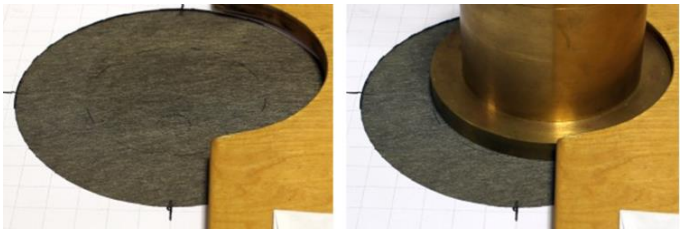

Fig. 33. Example of the SE measurement with use of F133 adapter

Measurement was performed for selected area of material sample for 5 adapter positions and a larger number of frequencies. These positions are selected on a circular area with a diameter of approximately 100 mm or 18.5 mm for measurement with use of the F133 adapter (fig. 33) or the F044 adapter (fig. 34) respectively. The location of the adapter on tested sample is determined with use of prepared template. The measurement result of the final measurement is the lowest value measured at each frequency for all positions of the adapter.

Fig. 34. Example of the SE measurement with use of F044 adapter

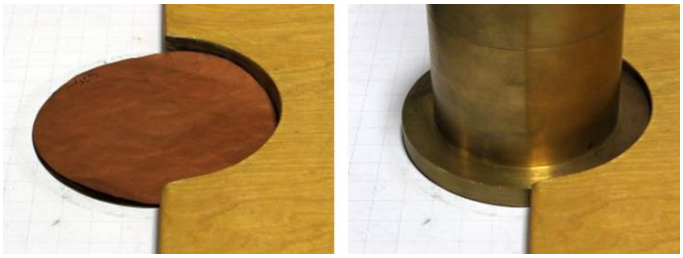

Fig. 35. Test setup used for dynamics measurement with use of F133 adapter

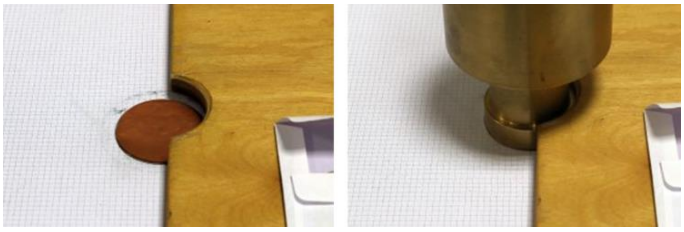

Fig. 36. Test setup used for dynamics measurement with use of F044 adapter

The dynamics of the measurement system was determined as SE measurement performed for two layers of copper foil with a thickness of 25 μm, which was used instead of the tested material sample. Examples of test setups are presented in fig. 35 and fig. 36.

D. Use of the GTEM

The GTEM cell, like other mentioned chambers, can be used for shielding effectiveness (SE) measurements of planar materials as well as small housing and cabinets for plain electromagnetic waves. The GTEM cell is used for generating incident field in a wide frequency range without transmit antennas. The SE of small-size planar material samples can be measured with use in the testing volume of the GTEM cell a small screened box (fig. 37 and 38). The screened box can be made from ventilation duct components (fig. 38, left). Its size should suffice to install inside them an element for measuring the field strength – a small receiving antenna, as well as the tested sample on one of its sides. An aperture – size of the hole in the small screened chamber – limits the lowest frequency of this test setup and other elements, especially SE characteristic of the small screened chamber, as well as the highest one and measuring dynamic range. The dynamic range (DR) is also limited by the transmit power and sensitivity of receiving side. A vector signal analyzer can be applied in this setup. To obtain higher DR power amplifiers in the transmitting path and the fiber optic link in the receiving path should be used.

The SE was determined also on the basis of equation (15) which allowed to apply the simplified testing procedure based on the one presented in previous subchapter. The S_{21} measurements were performed in three phases (fig. 39): without the tested material (reference measurement), repeated after the tested material installation and finalized with DR measurement of two layers of copper foil (each one with a thickness of 25 μm), which was used instead of the tested material sample. For measuring SE for an orthogonal polarization the sample of tested material has to be rotated by 90^0.

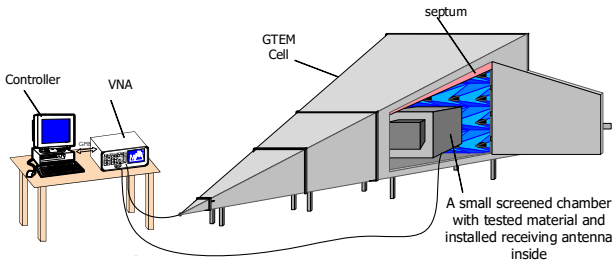

Fig. 37. An example of the test setup used for shielding effectiveness measurement with the use of the GTEM cell

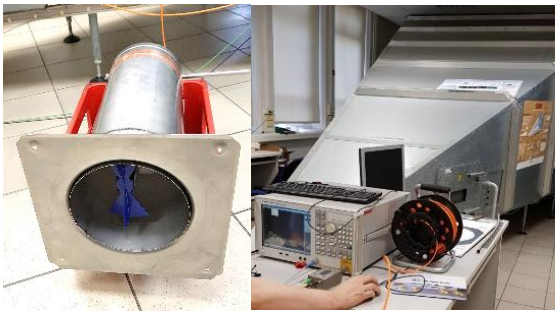

Fig. 38. The small screened box and the test setup for shielding effectiveness measurement with use of the GTEM cell and fiber optic link

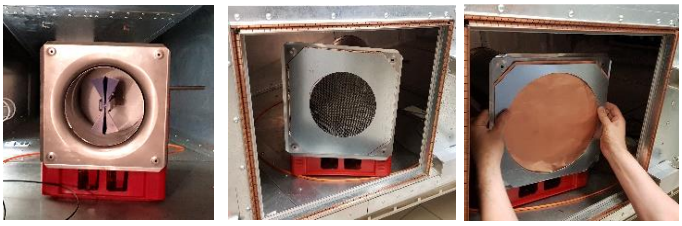

Fig. 39. Three phases of shielding effectiveness measurement with use of the GTEM cell: left) reference measurement, middle) with material sample, right) dynamic range

E. Use of the SAC method

The semi-anechoic chamber can be also used for shielding effectiveness (SE) measurements. It can be performed for much bigger and much heavier materials as well as housing and cabinets for plain electromagnetic waves. The SAC provides separation from the external electromagnetic environment as well as reduction of the electromagnetic wave reflection from walls and ceiling. The transmitting antenna is required to generate an electromagnetic field for tests (fig. 40). Measurements are performed separately for the magnetic or electric field, depending on used antenna types. Antennas have to be changed to cover a wider frequency range and tests have to be performed in subranges (i.e. up to 30 MHz for the magnetic field, 30MHz-1 GHz and 1-18 GHz and 18GHz – 40 GHz). A moveable screened chamber or barrier are necessary elements of test setup, too. This screened chamber's size is larger than in GTEM case, but limited by the SAC's main gate, because it has to be removed from the SAC for other EMC tests. It allows to install inside various receiving antennas and prepare larger aperture for SE testing. Samples may be much larger which in turn reduces the lowest testing frequency of this test setup. SE characteristic of the screened chamber and the cabling used limit the highest frequency and the measurement dynamic range. The dynamic range (DR) is also limited by the transmit power and sensitivity of the receiving side as well as the distance between transmitting and receiving antennas. A vector signal analyzer can be applied in this setup. To obtain higher DR than 70-80 dB power amplifiers in the transmitting path and a better shielding of the screened chamber should be used. To avoid unwanted couplings a fiber optic link in the receiving path is recommended. Test setups for SE measurement of cabinets and block made of concrete are presented in pictures fig. 41 and fig. 42 respectively.

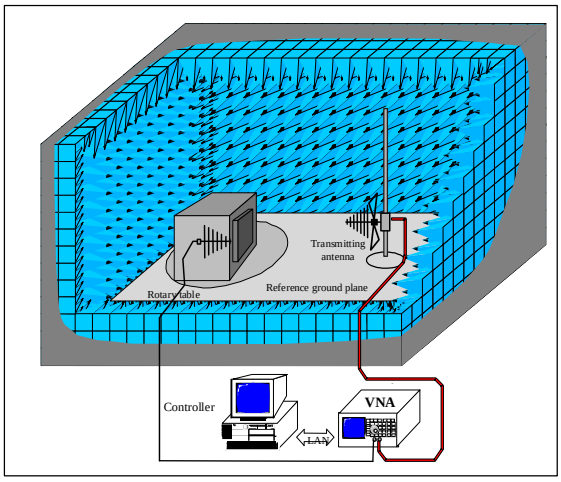

Fig. 40. An example of the test setup used for shielding effectiveness measurement of planar materials in the SAC

Fig. 41. An example of the test setup used for shielding effectiveness measurement of telecom cabinets in the SAC (up to 1 GHz)

The SE was determined with the same method as for measurements conducted in GTEM cell.

The S_{21} measurements were performed in the test setup without the tested material (a reference measurement), with installed material and with installed metal plate instead of the tested material sample (a dynamic range measurement). SE measurement for the orthogonal polarization were performed after receiving and testing antennas rotation (90^0).

Fig. 42. An example of the test setup used for shielding effectiveness measurement of steel mesh (left) and block of concrete (right) in the SAC

F. Presentation of results

Measurement setups with F133 and F044 adapters allowed for carrying out investigations on shielding effectiveness for over 300 samples, with dynamics obtained with these setups exceeding 100 dB. Outcomes are generated based on the measured *S* parameters, all of which are stored, which enables refining the methods in pace with appearance of new data processing algorithms.

In the investigations three characteristic material types were identified:

1. textiles with a conducting layer or conductive fibers. The material behaves similarly to perforated metal shields. Their shielding effectiveness deteriorates as a function of frequency;
2. materials with thin metal wires woven in. The materials have weak surface conductivity while their shielding effectiveness grows as a function of frequency;
3. materials with thin wires woven in forming a loose structure. Their shielding properties depend on the adapter clamping force. The material has resonant properties depending on the adapter aperture size and the material excitation place. The shielding effectiveness varies irregularly as a function of frequency, with different results yielded by different methods.

Measurement in the SAC allowed for carrying out investigations on the shielding effectiveness for over 30 large and heavy samples, mainly in the frequency range from 30 MHz up to 18 GHz with dynamics obtained with these setups exceeding 70 dB. A few cabinets were measured as well.

Detailed *SE* measurement results (*SE* - black line) obtained for exemplary samples are presented in fig. 43 through fig. 45. The figures demonstrate a dynamic range (*DR* – dotted grey line) as well as differences between maximum and minimum measured *SE* values (red bar graph), determined from measurements performed on 5 various adapter locations within a selected measuring area of a tested sample. If *DR* is not visible, it means that *DR* is higher than 100 dB.

The methodology described herein is presently being used in *round robin* tests, as a contribution to the IEEE P2715 project titled “Guide for the Characterization of the Shielding Effectiveness of Planar Materials”.

CONCLUSIONS

In the article the authors demonstrated the applicability of EMC laboratory for use cases other than those traditionally associated with this kind of facilities. Features such as controllability and stability of electromagnetic conditions achievable in these artificial environments make them indispensable in measurements of existing and emerging IoT radiocommunication systems. Due to the fact that these laboratories allow for obtaining considerable EM isolation from external interference and contain multiple internal mutually isolated chambers, it is possible to generate radio or cable channels for measuring ultrahigh-sensitivity systems capable of operating at extremely high dynamic power ranges. Moreover, the wide variety of chambers, spanning from anechoic and semi-anechoic through reverberation, enables emulating the channel impulse responses corresponding to different kinds of propagation environments, beginning with the free space (in anechoic chambers), open space (in the semi-anechoic chamber) and ending with indoor, micro- and macrocellular areas (by manipulating the reverberation chamber loading).

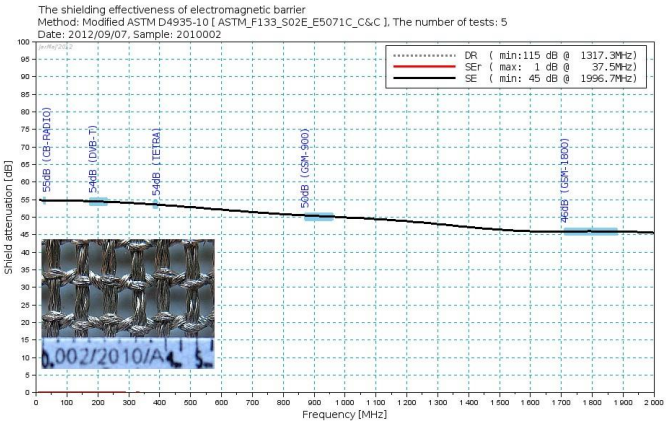

Fig. 43. An exemplary material of a mesh structure

The EMC facilities described herein can also be used for the transmission performance testing of various radio systems by emulating multipath propagation environments and providing separation from other radio systems and disturbances as well as for testing immunity of data transmission quality to electromagnetic disturbances. The reverberation chamber allows to create extraordinary multipath propagation environment for testing radio systems transmission quality and their ability to work in very challenging propagation conditions. Beside the above mentioned functionalities, semi-anechoic chambers allow for testing radio systems that offer ultimate transmission performance, implementing MIMO technology, especially short range radio systems.

Lastly, as was demonstrated in chapter IV, WUST ECL facilities lend themselves for use in investigations of shielding effectiveness of textiles and other materials. Results obtained to date have proven to be stable and highly repeatable. In connection with the authors’ own innovative measurement methodology developed for this purpose, opportunities have been created for considering WUST ECL as a reference laboratory for this sort of widely understood research on textiles electromagnetic properties. An example of measurement test results of the shielding effectiveness for a block of concrete (80 cm × 80 cm × 25 cm and weight more than 250 kg) is presented in the fig. 46.

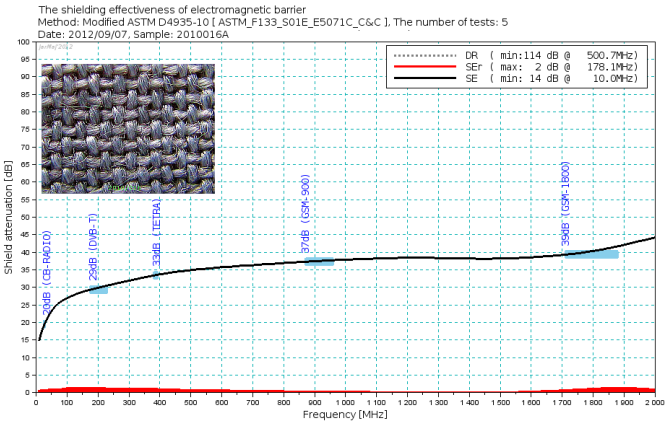

Fig. 44. An exemplary material of absorbing properties

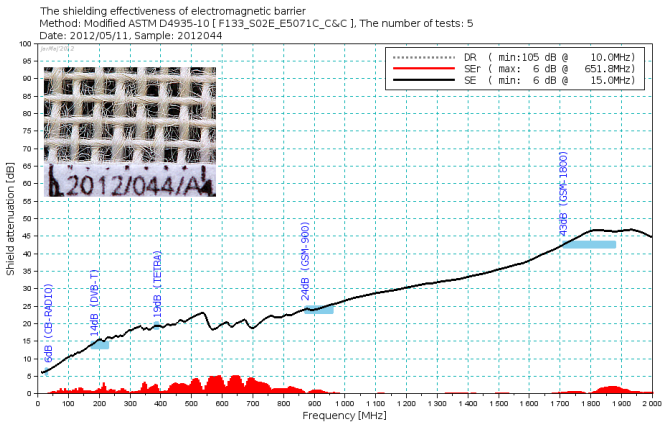

Fig. 45. An exemplary material of resonant properties

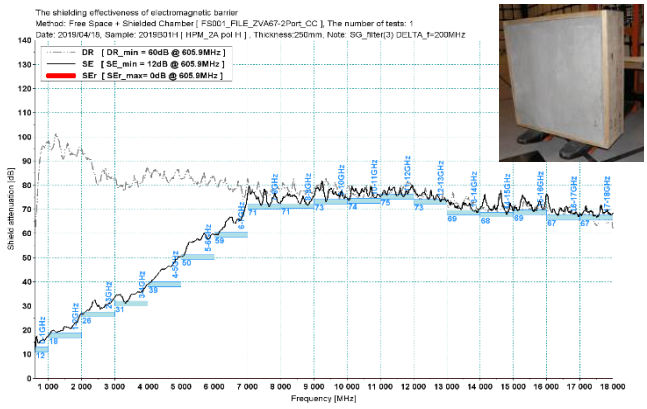

Fig. 46. SE of concrete block of 25 cm thickness measured with free space method in SAC with use of screened chamber

REFERENCES

[1] Low Throughput Networks (LTN); Use Cases for Low Throughput Networks, ETSI GS LTN 001 V1.1.1 (2014-09).

[2] Low Throughput Networks (LTN); Functional Architecture, ETSI GS LTN 002 V1.1.1 (2014-09).

[3] Low Throughput Networks (LTN); Protocols and Interfaces, ETSI GS LTN 003 V1.1.1 (2014-09).

[4] ETSI TR 103 435 V1.1.1 (2017-02), System Reference document (SRdoc); Short Range Devices (SRD); Technical characteristics for Ultra Narrow Band (UNB) SRDs operating in the UHF spectrum below 1 GHz.

[5] 3GPP TR 45.820, "Cellular System Support for Ultra Low Complexity and Low Throughput Internet of Things", V2.1.0, August, 2015.

[6] 3GPP TR 36.888, „Study on provision of low-cost Machine-Type Communications (MTC) User Equipments (UEs) based on LTE", v.12.0.0, June 2013.

[7] "The European table of frequency allocations and applications in the frequency range 8.3 kHz to 3000 GHz (ECA Table), appr. March 2019

[8] K. Staniec, M. Kowal, *LoRa performance under variable interference and heavy-multipath conditions*, Wireless Communications and Mobile Computing, 2018, vol. 2018, art. 6931083, pp. 1-9.

[9] A.J. Pomianek, K. Staniec, Z. Jóskiewicz, *Practical remarks on measurement and simulation methods to emulate the wireless channel in the reverberation chamber*, Progress in Electromagnetics Research-PIER. 2010, vol. 105, pp. 49-69.

[10] K. Staniec, *Evaluation of the ZigBee transmission repetition mechanism in the variably-loaded reverberation chamber*, Progress in Electromagnetics Research-PIER. 2012, vol. 132, pp. 297-314.

[11] Schelkunoff, S. A.: *Electromagnetic Waves*. Princeton. NJ: D. Van Nostrand, 1943

[12] Shulz, R. B.; Plantz, V. C. & Brush, D. R.: *Shielding theory and practice*, IEEE Trans. Electromagn. Compat., vol. 30, no. 3, pp. 187–201, Aug.1988.

[13] ASTM D4935-10, *Standard Test Method for Measuring the Electromagnetic Shielding Effectiveness of Planar Materials*, ASTM, 2010

[14] IEEE 299-2006,*IEEE Standard Method for Measuring the Effectiveness of Electromagnetic Shielding Enclosures*, IEEE, February 2007

[15] IEC 61000-4-21, *Electromagnetic compatibility (EMC) – Part 4-21: Testing and measurement techniques – Reverberation chamber test methods*, IEC, January 1, 2011

[16] Tadeusz W. Więckowski Jarosław M. Janukiewicz: *Methods for Evaluating the Shielding Effectiveness of Textiles*, FIBRES & TEXTILES in Eastern Europe January / December 2006, Vol. 14, No. 5 p.18-22.

[17] Jarosław Janukiewicz, *Kamień milowy M.9.4. Analiza efektywności metod badania skuteczności ekranowania materiałów barierowych PEM*, Report of Wroclaw University of Science and Technology, Wrocław 2013

[18] *Scilab free and open source software for numerical computation providing a powerful computing environment for engineering and scientific applications.* Version 5.5.2, Scilab Enterprises S.A.S, Released on 04/01/2015, Available: https://www.scilab.org/

[19] D.Hansen, P.Wilson, D.Königstein, and H.Schaer: *A broadband alternative EMC test chamber based on a TEM-cell anechoic-chamber hybrid concept*, Proceedings of the 1989 International Symposium on Electromagnetic Compatibility, pages 133-137, Nagoya, Japan, September 1989.

[20] EN 61000-4-20: *Electromagnetic compatibility (EMC) - Part 4-20: Testing and measurement techniques - Emission and immunity testing in transverse electromagnetic (TEM) waveguides*

[21] Emission and Immunity Measurements and Production of Best Practice Guide on GTEM Cells used for EMC measurements, National Physical Laboratory and York EMC Services Ltd, Final Report March 2003. PDF file available at www.npl.co.uk (Publications) and www.yorkemc.co.uk (Research).

[22] RTCA DO-160G (Dec. 8, 2010): *Environmental Conditions and Test Procedures for Airborne Equipment*

[23] CISPR 16-4-5 ed. 1 Amd.2 (Draft): *Specification of radio disturbance and immunity measuring apparatus and methods – Part 4-5: Uncertainties, statistics and limit modelling – Conditions for the use of alternative test methods*

[24] Makoto Hara, Yasuo Takahashi, Robert Vogt-Ardatjew, Frank Leferink: *Statistical Analysis for Reverberation Chamber with Flexible Shaking Walls with Various Amplitudes*, 2018 International Symposium on Electromagnetic Compatibility EMC EUROPE 2018, Amsterdam 27-30 August 2018

[25] R. Serra ; A. C. Marvin ; F. Moglie ; V. Mariani Primiani ; A. Cozza ; L. R. Arnaut ; Y. Huang ; M. O. Hatfield ; M. Klingler ; F. Leferink: *Reverberation chambers a la carte: An overview of the different mode-stirring techniques*, IEEE Electromagnetic Compatibility Magazine, 2017, Volume: 6, Issue: 1, pp. 63-78